

Extension of the fiber-free approach to complex stress-strain models for concrete

Francesco Marmo¹, Luciano Rosati¹

¹*Department of Structural Engineering, University of Naples Federico II, Naples, Italy*
E-mail: f.marmo@unina.it, rosati@unina.it

Keywords: Finite elements, nonlinear analysis, fiber methods.

SUMMARY. The fiber-free approach is a recently formulated methodology which has been conceived for the analytical integration of non-linear elastic and elasto-plastic normal stresses acting on beam cross sections. It is based on the use of analytical formulas which require the constitutive law to be integrated four times as a maximum and on the subdivision of the section in suitable subdomains, which are updated during the analysis of the structural model. Here we illustrate and apply a new approach for addressing partitions of the section which are defined by non-polygonal sides owing to the particularly involved expression of the stress-strain models; this typically occurs for the constitutive laws for concrete such as the ones due to Karsan-Jirsa or Mander et al., commonly employed in seismic engineering.

1 INTRODUCTION

Current seismic design recommendations assume that structures respond elastically only to small magnitude earthquakes but are expected to experience different degrees of damage during moderate and strong ground motions. Thus, in regions of high seismic risk, structures are required to respond inelastically to the maximum earthquake expected at the site during their usable life.

Recent efforts aiming at developing robust and reliable reinforced-concrete frame elements have focused, on one side, on more accurate element formulations [1], and on the other one, on the subdivision of elements into longitudinal fibers. This second aspect engenders two main advantages: first, the reinforced concrete section behaviour is derived from the uniaxial stress-strain behaviour of the fibers so that three-dimensional effects, such as concrete confinement by transverse steel, can be incorporated into the uniaxial stress-strain relation; second, the interaction between bending moment and axial force can be described accurately.

Within this framework an alternative method, the so called fiber-free approach, has been recently formulated [2] and successfully applied [3, 4] for integrating the stress field on the element sections when an elasto-plastic constitutive law, typically adopted in the non-linear static and dynamic analysis of reinforced concrete (RC) frames [5, 6], is adopted.

The fiber-free approach is based on the use of special formulas which allow one to compute exactly, for sections of arbitrary polygonal shape, the stress resultants of normal stresses and the relevant derivatives provided that the given expression of the constitutive law is amenable to be analytically integrated four times as a maximum. On the contrary, the traditional fiber approach is typically applied to sections composed of rectangles.

Moreover, considerable savings are obtained at the computational level since the history variables which need to be stored during a non-linear sectional analysis amount to some dozens since they are associated uniquely with the time-dependent partition of the section as function of the past history of deformation. Conversely, several thousands of history variables need to be stored in the fiber approach to achieve a degree of accuracy at least comparable with that permitted by the fiber-free approach [2].

However, the possibility of partitioning the section in polygonal subdomains, so as to apply the analytical integration formulas for each of them, depends on the particular constitutive model to address, namely on the function which express the plastic strain as a function of the maximum one attained during the past history at a given point of the section. Thus, polygonal subdomains are obtained e.g. for a bilinear constitutive model [2] while the same nice feature is not extended to the models proposed by Karsan and Jirsa [5] and by Mander, Priestley and Park [6] due to their particularly involved expressions.

In the original formulation [2] this problem was solved by adopting a piecewise linear interpolation of the non-linear function which generates each partition. Even if such approach engenders acceptable results [2, 3], it turns out to be relatively expensive from the computational point of view and, in some special cases, may cause unacceptable approximations when compared to the exactness of the results obtained by the use of analytical integration formulas.

For these reasons we here describe a new methodology which allows the user to address non-polygonal partitions so that a polygonal interpolation of such partition can be executed directly, without making use of piecewise linear interpolations of the constitutive function of the materials.

Some numerical results and comparisons with the fiber method are reported in order to show the correctness of the implementation and the advantages connected with the use of the proposed methodology with reference to the constitutive law originally proposed by Karsan and Jirsa [5], which is one of the most popular elasto-plastic constitutive models for concrete.

2 SECTIONAL ANALYSIS

A beam section Ω having a completely arbitrary polygonal shape is considered and a Cartesian reference frame, having origin at O , is introduced on the plane of the section; hence, each point of the section is identified by a two-dimensional position vector $\mathbf{r} = \{x, y\}$.

Furthermore an ordered set of n time parameters $t_0 < t_1 < \dots < t_n$ are considered and an historic analysis of the section is carried out by assuming that the current state of the section, which is relevant to the time parameter t^c , only depends on the states associated with previous time parameters $t < t_c$.

At a generic time t_k , the strain field on the section, which is assumed to be negative if compressive, is evaluated as:

$$\varepsilon^k(\mathbf{r}) = \varepsilon^k + \mathbf{g}^k \cdot \mathbf{r} \quad (1)$$

ε^k and $\mathbf{g}^k = (g_x^k, g_y^k)^t$ being the values that the strain at O and the curvature vector of the section attain at the generic time t_k , respectively; hence the current strain field on the section is also evaluated as $\varepsilon^c(\mathbf{r}) = \varepsilon^c + \mathbf{g}^c \cdot \mathbf{r}$.

As typically assumed for complex stress-strain models of concrete, the normal stress at a generic point \mathbf{r} of the section is expressed as a function of its current strain ε^c and of the maximum value ε_m^c that the compressive strain attains at \mathbf{r} during the past history of deformation of the section.

Such an assumption can be expressed symbolically as:

$$\sigma[\varepsilon^c(\mathbf{r}), \varepsilon_m^c(\mathbf{r})] = \begin{cases} e[\varepsilon^c(\mathbf{r})] & \varepsilon^c(\mathbf{r}) < \varepsilon_m^c(\mathbf{r}) \\ \frac{e[\varepsilon_m^c(\mathbf{r})]}{\varepsilon_m^c(\mathbf{r}) - \varepsilon_p[\varepsilon_m^c(\mathbf{r})]} \{\varepsilon^c - \varepsilon_p[\varepsilon_m^c(\mathbf{r})]\} & \varepsilon_m^c(\mathbf{r}) \leq \varepsilon^c(\mathbf{r}) < \varepsilon_p[\varepsilon_m^c(\mathbf{r})] \\ 0 & \varepsilon_p[\varepsilon_m^c(\mathbf{r})] \leq \varepsilon^c(\mathbf{r}) \end{cases} \quad (2)$$

where the functions $e(\cdot)$ and $\varepsilon_p(\cdot)$ are the envelope curve and the residual (plastic) strain, respectively; their actual expressions depend on the particular constitutive model associated with the points

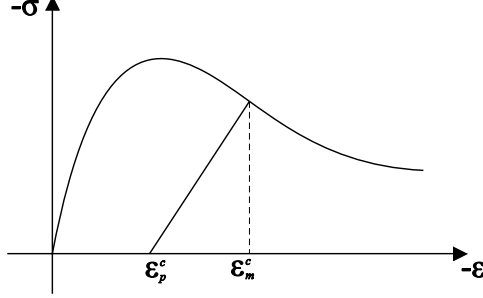


Figure 1: A typical uniaxial stress-strain law for concrete

of the section.

At a given point \mathbf{r} of the section the current and the maximum compressive strain attained at $t < t_c$ are univocally defined. According to the strain limits on the right-hand side of the constitutive function (2), only one among the three different expressions of the stress has to be applied to the considered point.

The resultants of the normal stresses acting on the section need to be evaluated in order to determine the axial force N and bending moment \mathbf{M} acting on the section at the current time:

$$N = \int_{\Omega} \sigma[\varepsilon^c(\mathbf{r}), \varepsilon_m^c(\mathbf{r})] dA; \quad \mathbf{M}^\perp = (-M_y, M_x)^t = \int_{\Omega} \sigma[\varepsilon^c(\mathbf{r}), \varepsilon_m^c(\mathbf{r})] \mathbf{r} dA \quad (3)$$

where the dependence of N and \mathbf{M} on the current strain parameters ε^c and \mathbf{g}^c and on the distribution of maximum compressive strain $\varepsilon_m^c(\mathbf{r})$ has been omitted for simplicity.

Finally, in order to carry out a nonlinear analysis based on a Newton-like strategy, we need to evaluate the derivatives of the resultant forces with respect to the current strain parameters ε^c and \mathbf{g}^c .

$$\mathbf{K}^c = \begin{bmatrix} \frac{\partial N}{\partial \varepsilon} \Big|_{\varepsilon^c} & \frac{\partial N}{\partial g_x} \Big|_{g_x^c} & \frac{\partial N}{\partial g_y} \Big|_{g_y^c} \\ -\frac{\partial M_y}{\partial \varepsilon} \Big|_{\varepsilon^c} & -\frac{\partial M_y}{\partial g_x} \Big|_{g_x^c} & -\frac{\partial M_y}{\partial g_y} \Big|_{g_y^c} \\ \frac{\partial M_x}{\partial \varepsilon} \Big|_{\varepsilon^c} & \frac{\partial M_x}{\partial g_x} \Big|_{g_x^c} & \frac{\partial M_x}{\partial g_y} \Big|_{g_y^c} \end{bmatrix} \quad (4)$$

3 THE FIBER-FREE APPROACH

Differently from the current strain $\varepsilon^c(\mathbf{r})$, the maximum compressive strain $\varepsilon_m^c(\mathbf{r})$ has not a unique expression over the whole section. This is due to the fact that the compressive strain is not maximized simultaneously at every point of the section. Consequently we first collect the points of the section where the maximum compressive strain is attained simultaneously, for instance at time t_i ; hence, the maximum compressive strain at such points can be evaluated as:

$$\varepsilon_m^c(\mathbf{r}) = \varepsilon^l(\mathbf{r}) = \varepsilon^l + \mathbf{g}^l \cdot \mathbf{r} \quad (5)$$

Accordingly, the strain parameters $\varepsilon_m^c = \varepsilon^l$ and $\mathbf{g}_m^c = \mathbf{g}^l$ are the ones which maximize the compressive strain on the considered set of points belonging to one of the subdomains of the section.

In order to determine the portion of the section, namely a partition [2], where each of the previous strain distributions maximizes the compressive strain, a cross-comparison between all the previous strain distributions is performed. Hence the generic partition Ω_l^c , evaluated at time t_c , is defined as the set of points of the section where a previous strain field ε_l maximizes the compressive strain:

$$\Omega_l^c = \{\mathbf{r} \in \Omega : \varepsilon^l(\mathbf{r}) < \varepsilon^k(\mathbf{r}), \forall t_k \neq t_l \text{ and } t_k, t_l < t_c\} \quad (6)$$

where t_k and t_l are two generic time parameters previous than the current one t_c .

Although the current strain and the maximum compressive strain are both expressed by means of an expression of the kind of formula (1) defined on Ω_l^c , the determination of the resultant forces and of their derivatives is still a difficult task due to the particular expression of the stress strain law (2). For this reason, in order to apply the integration formulas reported in [2] to the generic partition Ω_l^c , equation (2) is rewritten as follows:

$$\sigma[\varepsilon(\mathbf{r}), \varepsilon_m^c(\mathbf{r})] = h[\varepsilon_m^c(\mathbf{r})]\varepsilon^c + k[\varepsilon_m^c(\mathbf{r})] + l[\varepsilon^c(\mathbf{r})] \quad (7)$$

where $h(\cdot)$, $k(\cdot)$ and $l(\cdot)$ are three constitutive functions which are defined, as well as $\sigma(\cdot)$, by means of three expressions which are used alternatively depending on the value assumed by the strain. The advantage of using a constitutive function written in the form (7) is due to the fact that the three functions $h(\cdot)$, $k(\cdot)$ and $l(\cdot)$ depend only on one set of strain parameters; actually $h(\cdot)$ and $k(\cdot)$ depend just on the history strain parameters ε_m^c and \mathbf{g}_m^c , while $l(\cdot)$ depends only on the current strain parameters ε^c and \mathbf{g}^c . Finally the stress function is analytically integrated as a function of the values that the primitives of the functions $h(\cdot)$, $k(\cdot)$ and $l(\cdot)$ attain at the vertices of Ω_l^c .

4 THE NEW APPROACH FOR ADDRESSING NON-POLYGONAL PARTITIONS

According to the formulas (2) and (7), the stress distribution modifies as function of the parts of the section for which the different strain limits are attained. Thus, each partition Ω_l^c of the section needs to be further subdivided in order to apply the integration formulas referred to before. In this respect, we remind that the integration formulas provided in [2] can be used only for polygonal domains. However, the stress-strain laws for concrete which are typically employed in seismic engineering are characterized by nonlinear functions $\varepsilon_p[\varepsilon_m^c(\mathbf{r})]$ so that the portions Ω_{ij}^c of Ω_l^c which are determined by using $\varepsilon_p[\varepsilon_m^c(\mathbf{r})]$ as a limit for the strain value, are, in general, not polygonal. Consequently, in such cases, a polygonal approximation of Ω_{ij}^c is required.

To this end a polygonal interpolation Λ^c of the curve of equation $\varepsilon_p[\varepsilon_m^c(\mathbf{r})] = \varepsilon^c(\mathbf{r})$ is first determined by evaluating the position of its vertices λ_j^c . Subsequently, the intersections between Λ^c and the polygonal boundary $\partial\Omega_l^c$ of Ω_l^c are evaluated. Such intersections are then used to determine the vertices ω_{ij}^c of the boundary $\partial\Omega_{ij}^c$ of the partition (see Figure 2).

From now on we will always refer to the current time t_c so that, in order to simplify the notation, we will omit the superscript c .

4.1 The vertices of the polygon Λ

The vertices λ_j of the polygon Λ are requested to fulfill the condition:

$$\varepsilon_p[\varepsilon_m(\lambda_j)] = \varepsilon(\lambda_j) \quad \Rightarrow \quad \varepsilon_p(\varepsilon_m + \mathbf{g}_m \cdot \lambda_j) = \varepsilon + \mathbf{g} \cdot \lambda_j \quad (8)$$

Setting $\mathbf{g}_m^\perp = \{-g_{my}, g_{mx}\}^t$ and $\hat{\mathbf{g}}_m = \mathbf{g}_m/|\mathbf{g}_m|$ the position vector λ_j can be expressed in the reference system $(O, \hat{\mathbf{g}}_m, \hat{\mathbf{g}}_m^\perp)$ with $\hat{\mathbf{g}}_m^\perp = \mathbf{g}_m^\perp/|\mathbf{g}_m|$:

$$\lambda_j = \alpha_j \hat{\mathbf{g}}_m + \beta_j \hat{\mathbf{g}}_m^\perp \quad (9)$$

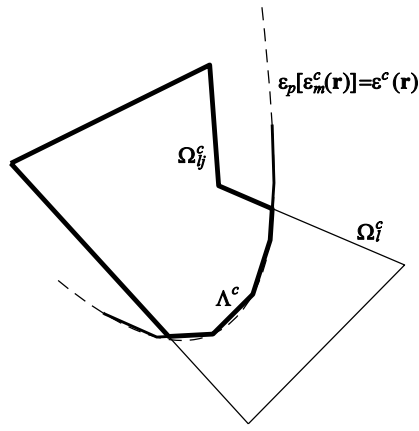


Figure 2: Polygonal interpolation of non-polygonal partitions

Since $\hat{\mathbf{g}}_m^\perp \cdot \mathbf{g}_m = 0$ and $\hat{\mathbf{g}}_m \cdot \mathbf{g}_m = |\mathbf{g}_m|$, substitution of the previous equation into (8) yields:

$$\varepsilon_p(\epsilon_m + |\mathbf{g}_m|\alpha_j) = \epsilon + \alpha_j \hat{\mathbf{g}}_m \cdot \mathbf{g} + \beta_j \hat{\mathbf{g}}_m^\perp \cdot \mathbf{g} \quad (10)$$

which can be easily solved for β_j :

$$\beta_j = \frac{\varepsilon_p(\epsilon_m + |\mathbf{g}_m|\alpha_j) - \epsilon - \alpha_j \hat{\mathbf{g}}_m \cdot \mathbf{g}}{\mathbf{g} \cdot \hat{\mathbf{g}}_m^\perp} \quad (11)$$

Consequently, setting an arbitrary value for α_j , the relevant value of β_j is evaluated by means of the previous equation and the position vector of the relevant vertex of Λ by means of equation (9).

In order to evaluate the terms of the stiffness matrix of the section, see equation (4), the derivatives of the vertices of Λ are also required. The derivatives of λ_j with respect to ϵ and \mathbf{g} are evaluated by applying the chain rule to equations (9) and (11) and considering that α_j has been assumed to be constant:

$$\lambda_{j,\epsilon} = \lambda_{j,\beta_j} \beta_{j,\epsilon} = \frac{\hat{\mathbf{g}}_m^\perp}{\mathbf{g} \cdot \hat{\mathbf{g}}_m^\perp} \quad (12)$$

and

$$\lambda_{j,\mathbf{g}} = \lambda_{j,\beta_j} \otimes \beta_{j,\mathbf{g}} = \hat{\mathbf{g}}_m^\perp \otimes \beta_{j,\mathbf{g}} \quad (13)$$

where

$$\beta_{j,\mathbf{g}} = \frac{-\alpha_j \hat{\mathbf{g}}_m (\mathbf{g} \cdot \hat{\mathbf{g}}_m^\perp) + \hat{\mathbf{g}}_m^\perp [\varepsilon_p(\epsilon_m + |\mathbf{g}_m|\alpha_j) - \epsilon - \alpha_j \hat{\mathbf{g}}_m \cdot \mathbf{g}]}{(\mathbf{g} \cdot \hat{\mathbf{g}}_m^\perp)^2} \quad (14)$$

The case $\mathbf{g} \cdot \hat{\mathbf{g}}_m^\perp = 0$ also needs to be considered since the denominator of formula (11) is zero. Actually, in such a situation equation (10) specializes to:

$$\varepsilon_p(\epsilon_m + |\mathbf{g}_m|\alpha_j) = \epsilon + \alpha_j \hat{\mathbf{g}}_m \cdot \mathbf{g} \quad (15)$$

and needs to be solved for α_j . For brevity we omit the details of such procedure.

4.2 Intersections between Λ and $\partial\Omega_l$

The evaluation of the coordinates of the intersections between $\partial\Omega_l$ and Λ is carried out by intersecting the sides of $\partial\Omega$ and Λ one each other. To this end, a loop over the sides of $\partial\Omega$ is executed and, for each of the sides of $\partial\Omega$, a nested loop over the sides of Λ is performed.

At the generic i -th - j -th step of such a nested loop, intersection between the i -th side of $\partial\Omega$ and the j -th side of Λ is evaluated as described below.

The generic point of the i -th side of $\partial\Omega$ has coordinates:

$$\boldsymbol{\omega}(w_i) = \boldsymbol{\omega}_i + w_i(\boldsymbol{\omega}_{i+1} - \boldsymbol{\omega}_i); \quad 0 \leq w_i \leq 1 \quad (16)$$

where $\boldsymbol{\omega}_i$ and $\boldsymbol{\omega}_{i+1}$ are the two end points of such segment.

Similarly, the generic point of the j -th side of Λ has coordinates:

$$\boldsymbol{\lambda}(l) = \boldsymbol{\lambda}_j + l_j(\boldsymbol{\lambda}_{j+1} - \boldsymbol{\lambda}_j); \quad 0 \leq l_j \leq 1 \quad (17)$$

where $\boldsymbol{\lambda}_j$ and $\boldsymbol{\lambda}_{j+1}$ are the two end points of the considered side.

The intersection between these two sides, if it exists, is determined by solving for w_i and l_j the equation:

$$\boldsymbol{\omega}_i + w_i(\boldsymbol{\omega}_{i+1} - \boldsymbol{\omega}_i) = \boldsymbol{\lambda}_j + l_j(\boldsymbol{\lambda}_{j+1} - \boldsymbol{\lambda}_j) \quad (18)$$

provided that the conditions $0 \leq w_i \leq 1$ and $0 \leq l_j \leq 1$ are fulfilled.

In order to solve equation (18), both sides of (18) are scalarly multiplied by $(\boldsymbol{\lambda}_{j+1}^\perp - \boldsymbol{\lambda}_j^\perp)$ and then the resulting equation is solved for w_i , yielding:

$$\bar{w}_{ij} = \frac{\boldsymbol{\lambda}_j \cdot \boldsymbol{\lambda}_{j+1}^\perp - \boldsymbol{\omega}_i \cdot (\boldsymbol{\lambda}_{j+1}^\perp - \boldsymbol{\lambda}_j^\perp)}{(\boldsymbol{\omega}_{i+1} - \boldsymbol{\omega}_i) \cdot (\boldsymbol{\lambda}_{j+1}^\perp - \boldsymbol{\lambda}_j^\perp)} \quad (19)$$

Similarly, by scalarly multiplying for $(\boldsymbol{\omega}_{i+1}^\perp - \boldsymbol{\omega}_i^\perp)$ both sides of (18), and then solving for l_j , one gets:

$$\bar{l}_{ij} = \frac{\boldsymbol{\omega}_i \cdot \boldsymbol{\omega}_{i+1}^\perp - \boldsymbol{\lambda}_j \cdot (\boldsymbol{\omega}_{i+1}^\perp - \boldsymbol{\omega}_i^\perp)}{(\boldsymbol{\lambda}_{j+1} - \boldsymbol{\lambda}_j) \cdot (\boldsymbol{\omega}_{i+1}^\perp - \boldsymbol{\omega}_i^\perp)} \quad (20)$$

Whenever the previous two equations are not defined, i.e. when:

$$(\boldsymbol{\omega}_{i+1} - \boldsymbol{\omega}_i) \cdot (\boldsymbol{\lambda}_{j+1}^\perp - \boldsymbol{\lambda}_j^\perp) = -(\boldsymbol{\lambda}_{j+1} - \boldsymbol{\lambda}_j) \cdot (\boldsymbol{\omega}_{i+1}^\perp - \boldsymbol{\omega}_i^\perp) = 0 \quad (21)$$

the two segments $[\boldsymbol{\omega}_i, \boldsymbol{\omega}_{i+1}]$ and $[\boldsymbol{\lambda}_j, \boldsymbol{\lambda}_{j+1}]$ are parallel one each other and the intersection does not exist.

If both solutions (19) and (20) fulfill the conditions $0 \leq \bar{w}_{ij} \leq 1$ and $0 \leq \bar{l}_{ij} \leq 1$, respectively, the intersection has coordinates:

$$\mathbf{i}_{ij} = \boldsymbol{\omega}_i + \bar{w}_{ij}(\boldsymbol{\omega}_{i+1} - \boldsymbol{\omega}_i) \quad (22)$$

or alternatively:

$$\mathbf{i}_{ij} = \boldsymbol{\lambda}_j + \bar{l}_{ij}(\boldsymbol{\lambda}_{j+1} - \boldsymbol{\lambda}_j) \quad (23)$$

Denoting by $\boldsymbol{\omega}_{i,\epsilon}$, $\boldsymbol{\omega}_{i,\mathbf{g}}$, $\boldsymbol{\omega}_{i+1,\epsilon}$ and $\boldsymbol{\omega}_{i+1,\mathbf{g}}$ the derivatives of the end points of the i -th side of $\partial\Omega$ with respect to ϵ and \mathbf{g} , and by $\boldsymbol{\lambda}_{j,\epsilon}$, $\boldsymbol{\lambda}_{j,\mathbf{g}}$, $\boldsymbol{\lambda}_{j+1,\epsilon}$ and $\boldsymbol{\lambda}_{j+1,\mathbf{g}}$ the same derivatives of the two endpoints of the j -th side of Λ , we now proceed to evaluate the derivatives of the intersection between these two sides.

The derivative of equation (22) with respect to ϵ is:

$$\mathbf{i}_{ij,\epsilon} = \boldsymbol{\omega}_{i,\epsilon} + \bar{w}_{ij,\epsilon}(\boldsymbol{\omega}_{i+1} - \boldsymbol{\omega}_i) + \bar{w}_{ij}(\boldsymbol{\omega}_{i+1,\epsilon} - \boldsymbol{\omega}_{i,\epsilon}) \quad (24)$$

where $\bar{w}_{ij,\epsilon}$ is evaluated by differentiating equation (19):

$$\begin{aligned} \bar{w}_{ij,\epsilon} = & \{ [(\boldsymbol{\omega}_{i+1} - \boldsymbol{\omega}_i) \cdot (\boldsymbol{\lambda}_{j+1}^\perp - \boldsymbol{\lambda}_j^\perp)] [\boldsymbol{\lambda}_{j,\epsilon} \cdot \boldsymbol{\lambda}_{j+1}^\perp + \boldsymbol{\lambda}_j \cdot \boldsymbol{\lambda}_{j+1,\epsilon}^\perp + \\ & - \boldsymbol{\omega}_{i,\epsilon} \cdot (\boldsymbol{\lambda}_{j+1}^\perp - \boldsymbol{\lambda}_j^\perp) - \boldsymbol{\omega}_i \cdot (\boldsymbol{\lambda}_{j+1,\epsilon}^\perp - \boldsymbol{\lambda}_{j,\epsilon}^\perp)] + \\ & - [\boldsymbol{\lambda}_j \cdot \boldsymbol{\lambda}_{j+1}^\perp - \boldsymbol{\omega}_i \cdot (\boldsymbol{\lambda}_{j+1}^\perp - \boldsymbol{\lambda}_j^\perp)] [(\boldsymbol{\omega}_{i+1,\epsilon} - \boldsymbol{\omega}_{i,\epsilon}) \cdot (\boldsymbol{\lambda}_{j+1}^\perp - \boldsymbol{\lambda}_j^\perp) + \\ & - (\boldsymbol{\omega}_{i+1} - \boldsymbol{\omega}_i) \cdot (\boldsymbol{\lambda}_{j+1,\epsilon}^\perp - \boldsymbol{\lambda}_{j,\epsilon}^\perp)] \} / [(\boldsymbol{\omega}_{i+1} - \boldsymbol{\omega}_i) \cdot (\boldsymbol{\lambda}_{j+1}^\perp - \boldsymbol{\lambda}_j^\perp)]^2 \end{aligned} \quad (25)$$

Similarly, differentiating equation (22) with respect to \mathbf{g} one gets:

$$\mathbf{i}_{ij,\mathbf{g}} = \boldsymbol{\omega}_{i,\mathbf{g}} + (\boldsymbol{\omega}_{i+1} - \boldsymbol{\omega}_i) \otimes \bar{w}_{ij,\mathbf{g}} + \bar{\lambda}_{ij}(\boldsymbol{\omega}_{i+1,\mathbf{g}} - \boldsymbol{\omega}_{i,\mathbf{g}}) \quad (26)$$

where:

$$\begin{aligned} \bar{w}_{ij,\mathbf{g}} = & \{ [(\boldsymbol{\omega}_{i+1} - \boldsymbol{\omega}_i) \cdot (\boldsymbol{\lambda}_{j+1}^\perp - \boldsymbol{\lambda}_j^\perp)] [\boldsymbol{\lambda}_{j,\mathbf{g}}^t \cdot \boldsymbol{\lambda}_{j+1}^\perp + \boldsymbol{\lambda}_{j+1,\mathbf{g}}^{\perp t} \cdot \boldsymbol{\lambda}_j^t + \\ & - \boldsymbol{\omega}_{i,\mathbf{g}}^t \cdot (\boldsymbol{\lambda}_{j+1}^\perp - \boldsymbol{\lambda}_j^\perp) - (\boldsymbol{\lambda}_{j+1,\mathbf{g}}^{\perp t} - \boldsymbol{\lambda}_{j,\mathbf{g}}^{\perp t}) \cdot \boldsymbol{\omega}_i] + \\ & - [\boldsymbol{\lambda}_j \cdot \boldsymbol{\lambda}_{j+1}^\perp - \boldsymbol{\omega}_i \cdot (\boldsymbol{\lambda}_{j+1}^\perp - \boldsymbol{\lambda}_j^\perp)] [(\boldsymbol{\omega}_{i+1,\mathbf{g}}^t - \boldsymbol{\omega}_{i,\mathbf{g}}^t) \cdot (\boldsymbol{\lambda}_{j+1}^\perp - \boldsymbol{\lambda}_j^\perp) + \\ & - (\boldsymbol{\lambda}_{j+1,\mathbf{g}}^{\perp t} - \boldsymbol{\lambda}_{j,\mathbf{g}}^{\perp t}) \cdot (\boldsymbol{\omega}_{i+1} - \boldsymbol{\omega}_i)] \} / [(\boldsymbol{\omega}_{i+1} - \boldsymbol{\omega}_i) \cdot (\boldsymbol{\lambda}_{j+1}^\perp - \boldsymbol{\lambda}_j^\perp)]^2 \end{aligned} \quad (27)$$

5 AN APPLICATION TO THE KARSAN-JIRSA CONSTITUTIVE LAW

In order to ensure the effectiveness of the new partitioning approach applied to the fiber-free method, several numerical tests have been carried out by comparing the results entailed by the proposed approach with those associated with the use of the well-known fiber method. In this section we also investigate on the degree of approximation introduced by the adoption of the fiber method, so pervasively used for integrating elastic-plastic normal stress fields. As a representative example of the numerical tests which have been performed, we illustrate the results obtained for a rectangular section of size $0.40 \times 0.60 [m^2]$ made of the material described in [3] with $f'_c = 35 [MPa]$ and $\varepsilon_{co} = 0.0017$. The section has been analyzed by setting $\epsilon = 0$, while it has been set $g_x = 0.5 \times g_y$ with g_y first increased from 0 to $0.02625 [m^{-1}]$ and subsequently decreased to $0.01875 [m^{-1}]$ by adopting steps of $0.00125 [m^{-1}]$. The relevant $M_y - g_y$ curve obtained by the fiber-free approach is plotted in Figure 3.

The results obtained with the fiber-free approach have been compared with the ones obtained by the fiber method by progressively increasing the number of fibers up to 2.4×10^4 ; in particular, the results reported below have been obtained by assuming a number of fibers equal to 4×6 , 8×12 , 16×24 , 32×48 , 64×96 , 128×192 , respectively.

In order to estimate the discrepancy between the results of the fiber method and those of the fiber-free approach, we defined the following parameter:

$$e(x) = \frac{x - x_o}{x_o} \quad (28)$$

where the quantity x is the one evaluated by means of the fiber method, while x_o is the corresponding one evaluated by the fiber-free approach.

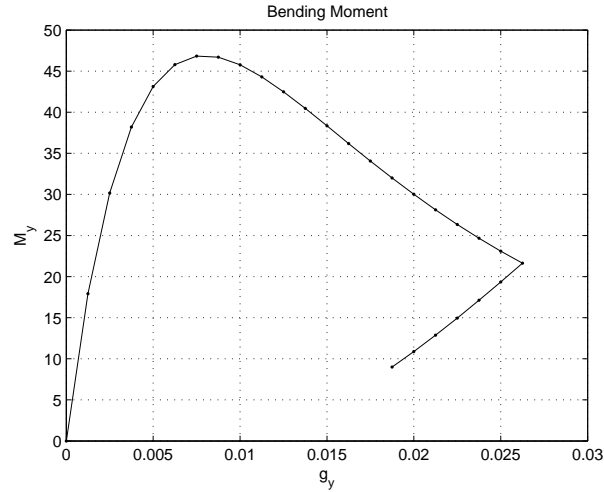


Figure 3: $M_y - g_y$ curve obtained by the fiber-free approach

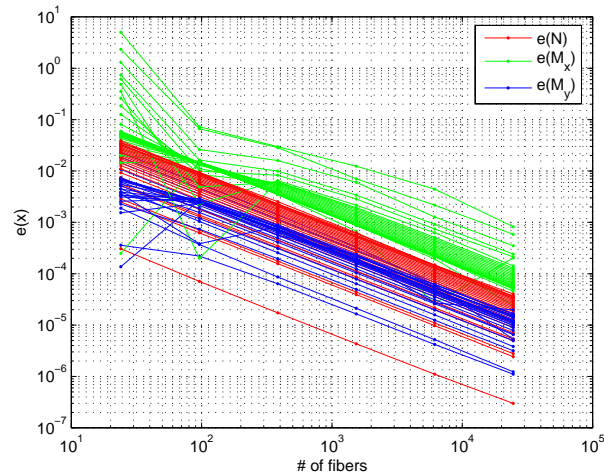


Figure 4: Discrepancy parameter vs. number of fibers: resultant forces

For each of the points of the $M_y - g_y$ curve of Figure 3, the values of $e(x)$ relevant to the evaluation of the resultant forces and the entries of the stiffness matrix are reported in Figures 4-7 in bi-logarithmic charts.

From these four plots the following conclusions can be drawn:

1) The parameter $e(x)$ tends to zero as the number of fibers tends to infinity, meaning that the results obtained by the fiber method converge to the ones obtained by the fiber-free approach as the number of fibers is increased. Such result confirms the accuracy of the results obtained by the

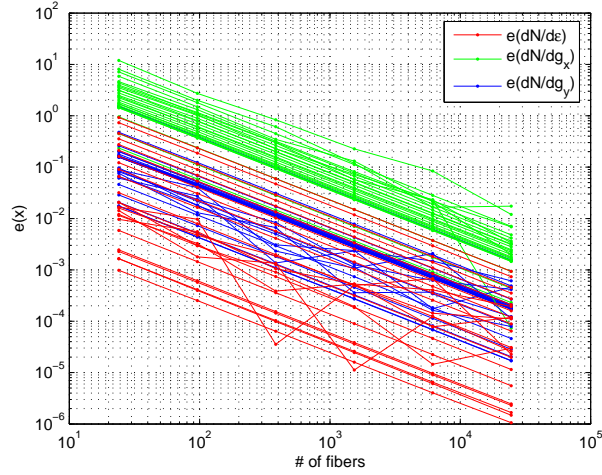


Figure 5: Discrepancy parameter vs. number of fibers: derivatives of N

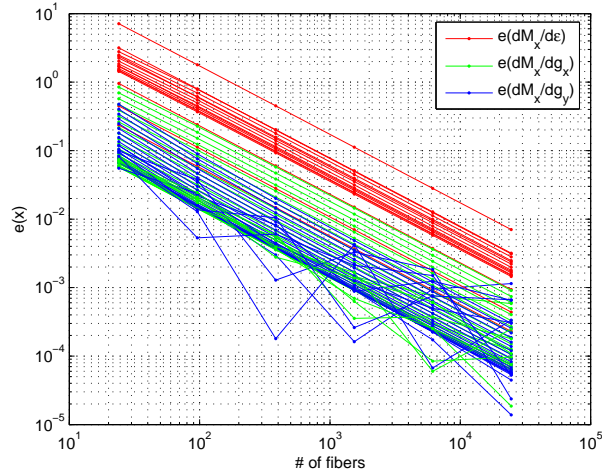


Figure 6: Discrepancy parameter vs. number of fibers: derivatives of M_x

fiber-free approach and the correctness of the implementation of both methods.

2) The rate of convergence of the fiber method relevant to the evaluation of the resultant forces is greater than the one relevant to the evaluation of the stiffness matrix. For instance, while 96 fibers are sufficient to lower the value of $e(N)$ to 10^{-2} , more than 1.5×10^3 fibers are needed to obtain the same result for $e(N, \epsilon)$.

3) When a very low number of fibers (less than 10^3) is used to discretize the section, the discrepancy parameter relevant to the evaluation of the stiffness matrix might be greater than 10; such an

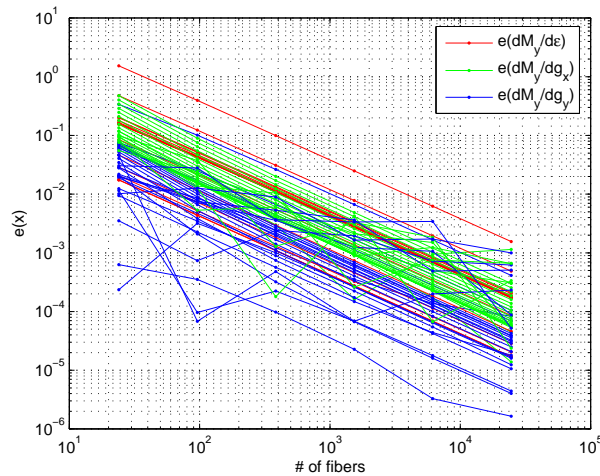


Figure 7: Discrepancy parameter vs. number of fibers: derivatives of M_y

unexpectedly high value means that, in such cases, the results of the fiber method and those of the fiber-free approach barely coincide in magnitude.

References

- [1] Neuenhofer, A., Filippou, F. C., Evaluation of Nonlinear Frame Finite-Element Models, in *ASCE Journal of Structural Engineering* **123**(7), 958-966 (1997)
- [2] Marmo, F., A Fiber-Free approach to the inelastic analysis of reinforced concrete structures, *University of Naples, Federico II, Doctoral Thesis*, (2008)
- [3] Marmo, F., Rosati, L., Incorporation of the Karsan-Jirsa model within the Fiber-Free approach, in *Proceedings of ReLUIS*, Roma, May 29th-30th, (2008)
- [4] Marmo, F., Rosati, L., Sessa, S., Exact integration of uniaxial elasto-plastic laws for nonlinear structural analysis, in *Proceedings of 2008 Seismic Engineering Conference commemorating the 1908 Messina and Reggio Calabria Earthquake*, Reggio Calabria, Italy, July 8th-11th, (2008)
- [5] Karsan, I. D., Jirsa, J. O., Behavior of concrete under compressive loading, in *Journal of Structural Division ASCE*, **95**(ST12), 2543-2563, (1969)
- [6] Mander, J. B., Priestley, M. J. N., Park, R., Theoretical stress-strain model for confined concrete, in *Journal of Structural Engineering ASCE*, **114**(8), 1804-1825, (1988)